Ozone climatology using interactive chemistry: results from the Canadian Middle Atmosphere Model

JOURNAL OF GEOPHYSICAL RESEARCH, VOL. 105, NO. D21, PAGES 26,475–26,491, NOVEMBER 16, 2000

Ozone climatology using interactive chemistry: Results from the Canadian Middle Atmosphere Model

J. de Grandpré, S. R. Beagley, V. I. Fomichev, E. Griffioen,
J. C. McConnell, and A. S. Medvedev

Department of Earth and Atmospheric Science, York University, Toronto, Ontario, Canada

T. G. Shepherd

Department of Physics, University of Toronto, Toronto, Ontario, Canada

Abstract. The climatology of ozone produced by the Canadian Middle Atmosphere Model (CMAM) is presented. This three-dimensional global model incorporates the radiative feedbacks of ozone and water vapor calculated on-line with a photochemical module. This module includes a comprehensive gas-phase reaction set and a limited set of heterogeneous reactions to account for processes occurring on background sulphate aerosols. While transport is global, photochemistry is solved from about 400 hPa to the top of the model at ~95 km. This approach provides a complete and comprehensive representation of transport, emission, and photochemistry of various constituents from the surface to the mesopause region. A comparison of model results with observations indicates that the ozone distribution and variability are in agreement with observations throughout most of the model domain. Column ozone annual variation is represented to within 5-10% of the observations except in the Southern Hemisphere for springtime high latitudes. The vertical ozone distribution is generally well represented by the model up to the mesopause region. Nevertheless, in the upper stratosphere, the model generally underestimates the amount of ozone as well as the latitudinal tilting of ozone isopleths at high latitude. Ozone variability is analyzed and compared with measurements. The comparison shows that the phase and amplitude of the seasonal variation as well as shorter timescale variations are well represented by the model at various latitudes and heights. Finally, the impact of incorporating ozone radiative feedback on the model climatology is isolated. It is found that the incorporation of ozone radiative feedback results in a cooling of ~8 K in the summer stratopause region, which corrects a warm bias that results when climatological ozone is used.

1. Introduction

Global modeling of ozone is essential to address climate issues such as ozone trends [*World Meteorological Organization (WMO)*, 1999]. To understand the details of such phenomena, it is necessary to use comprehensive modeling tools that can incorporate a multitude of processes and interactions, including atmospheric interannual variability, to study the potential causes and significance of natural and anthropogenic perturbations. It is also necessary to consider the atmosphere as a global system and to address questions about long–term coupling mechanisms between the various regions which become important over timescales of several decades. Ozone is dependent on a large number of atmospheric constituents, each with their own photochemical and transport characteristics, which allows for a multitude of indirect effects. Ozone is also at the heart of very important feedbacks between transport, radiation, and photochemistry, and its own distribution needs to be carefully represented given its role in the balance between important forcing mechanisms.

Middle atmosphere models (MAMs) are powerful tools to incorporate, directly or via parameterizations, the various processes which are considered to be important to address such issues. However, these models are also computationally expensive, complex, and suffer from major limitations in terms of their representation of subgrid–scale processes. Currently, an important source of uncertainty for MAMs concerns the role played by gravity–wave drag (GWD) processes. Their effects are generally included via parameterization schemes and can affect, directly or indirectly, important features observed in species distributions. In

Paper number 2000JD900427.
0148-0227/00/2000JD900427$09.00

polar regions the direct impact on ozone can be particularly important given the role GWD plays in the determination of the meridional circulation and consequently on the strength and evolution of the polar vortices [*Garcia and Boville,* 1994]. Other problem areas in MAMs include issues which are associated with the representation of tropical ascent, subtropical mixing barriers [*Mote et al.,* 1996; *Volk et al.,* 1996], and the lack of a proper representation of the quasi–biennial oscillation [*WMO,* 1999, chap. 7].

In spite of these difficulties, the implementation of comprehensive chemical schemes into MAMs in an interactive manner is now seen as being important for climate studies. Recent studies have shown that MAMs can successfully incorporate comprehensive photochemistry modules to reproduce several basic characteristics of the ozone stratospheric climatology [e.g., *Eckman et al.,* 1995; *Rasch et al.,* 1995]. Such models, and others using parameterized photochemistry, have been already employed to investigate ozone depletion scenarios and climate–related issues such as dilution effects [e.g., *Cariolle et al.,* 1990; *Eckman et al.,* 1996]. The Canadian Middle Atmosphere Model utilizes a comprehensive approach whereby prognostic ozone is calculated and used every time step to calculate radiative processes. The transport of long–lived species is applied over the full model domain which includes the troposphere, the mesosphere, and the lower thermosphere. The use of a higher lid (~95 km) than is traditional allows for a more complete representation of the middle atmosphere transport which determines the distribution of key constituents such as methane, nitrous oxide, and water vapor. It also provides the opportunity of imposing species boundary conditions farther away from the stratosphere.

The ozone distribution in the stratosphere is also strongly influenced by processes occurring in the troposphere since the stratospheric abundances of nitrogen oxides and halogens are determined by the emission and transport of their tropospheric precursors. It is thus important to extend the calculation of the photochemistry to the upper troposphere in order to maintain adequate lower boundary conditions. Ultimately, it will be important to have a model where the complex chemistry of the troposphere is also coupled into MAMs. Such a model could potentially be used to address other important issues such as the effects of aircraft (both subsonic and supersonic) on ozone and climate, and the impact of ozone changes at the tropopause on surface temperatures. Such a model would require a more detailed and accurate representation of the chemistry and dynamics, and in particular, of stratosphere–troposphere exchange processes [*Intergovernmental Panel on Climate Change (IPCC),* 1999].

In this paper, we present results from a multiyear integration of the model and compare them with a reference climatology in various regions. We demonstrate that the overall approach to simulate ozone within an extended domain produces a good representation of the ozone distribution and variability over a wide range of spatio–temporal scales. The paper highlights the model's capability to incorporate various feedbacks and forcing mechanisms. Some discussion on potential model improvements in various areas is also presented.

2. Model Description

The Canadian Middle Atmosphere Model (CMAM) is a vertically extended and modified version of the general circulation model (GCM) of the Canadian Centre for Climate Modelling and Analysis (CCCma) [*McFarlane et al.,* 1992]. It is a spectral model with a hybrid vertical coordinate which is terrain following near the surface and changes to a pressure coordinate throughout the middle atmosphere. This version of the model is run with 50 levels and T32 spectral resolution in the horizontal and uses a 15–min time step. In the middle atmosphere the vertical resolution is ~3 km, and the model top is at $p = 0.000637$ hPa or about 95 km. The climatology of the earlier version of the CMAM was described by *Beagley et al.* [1997], and preliminary results with the chemical module were presented by *de Grandpré et al.* [1997]. To describe the momentum deposition by a broad spectrum of subgrid-scale gravity waves (GWs), the parameterization scheme of *Medvedev and Klaassen* [1995] is used. In this study, the GW source is represented by an isotropic wave spectrum launched near the tropopause as described by *Medvedev et al.* [1998]. For orographic GWs the parameterization of *McFarlane* [1987] is used. We also employ the middle atmosphere infrared scheme from *Fomichev and Blanchet* [1995] and *Fomichev et al.* [1998].

The model includes a photochemistry module which contains 44 species including odd–hydrogen, odd–nitrogen, odd-chlorine, and odd-bromine families, N_2O, CFC-11, and CFC-12, CH_3Br, CH_4, and its oxidation products including CO. It has 127 photochemical reactions, including 34 photolysis reactions, for which the data are taken from *DeMore et al.* [1994] unless otherwise noted. Photochemical reactions added since the earlier report [*de Grandpré et al.,* 1997] are listed in Table 1 and are commented on below. Transport is active throughout the domain, while chemistry is solved on-line from ~6 km to the top of the model. For this model version a spectral advection scheme is used for the transport of moisture and other chemical constituents. A full diurnal cycle is simulated with photolysis rates provided by a lookup table. The chemistry solver is a mass-conserving fully implicit backward difference scheme [*Sandilands and McConnell,* 1997].

Changes from the previous report include the transport of the chlorofluorocarbons and the addition of atomic nitrogen and methyl bromide (CH_3Br). Although not all forms of stratospheric chlorine and bromine have been included, the mixing ratios for both CH_3Br and the CFCs have been adjusted so that the

Table 1. New Gas-Phase Photochemical Reactions

Reaction No.	Reaction		
(R1)	$N + NO$	$\longrightarrow$	$N_2 + O$
(R2)	$N + OH$	$\longrightarrow$	$NO + H$
(R3)	$N + O_2$	$\longrightarrow$	$NO + O$
(R4)	$N + HO_2$	$\longrightarrow$	$OH + NO$
(R5)	$CH_3Br + OH + O_2$	$\longrightarrow$	$Br + CO + 2H_2O$
(R6)	$CH_3Br + O(^1D) + O_2$	$\longrightarrow$	$OH + H_2O + CO + BrO$
(R8)	$NO + h\nu$	$\longrightarrow$	$N + O$
(R9)	$CH_3Br + h\nu$	$\longrightarrow$	$OH + BrO + CO + H_2O$

chlorine and bromine loading of the stratosphere is appropriate for mid-1990s conditions. The halogen reservoir is maintained at 3.5 ppbv by imposing CFC-11 and CFC-12 surface mixing ratios at 0.55 ppbv and 0.93 ppbv, respectively. For methyl bromide a value of 14 parts per trillion by volume (pptv) has been used to include other sources of bromine which have not been taken into account. As before, nitrous oxide and methane have their surface values specified as 315 ppbv and 1.6 ppmv, respectively. To prevent the long-term buildup of other transported species, a dry deposition term with a deposition velocity of 0.3 cm s^{-1} is applied.

The addition of nitrogen atom chemistry to the model has been made to improve the NO_x distribution in the mesosphere. Thus the photolysis of NO followed by the reaction of the N formed with the remaining NO, which represents the main sink for odd–nitrogen in the mesosphere and lower thermosphere, has been added along with a few other reactions involving atomic nitrogen (see Table 1). Additionally, upper boundary conditions for odd–oxygen and odd–nitrogen of 0.01 volume mixing ratio and 1 ppmv, respectively, have been applied to account for the flux of these species to and from the lower thermosphere. The description of tropospheric processes has been improved by the addition of convective mixing using a mass flux scheme [*Zhang and McFarlane,* 1995] together with a shallow convective mixing scheme based on convective adjustment [*Abdella and McFarlane,* 1996].

Photolysis values are computed by a table lookup method; the current variables against which the interpolation is done are height, solar zenith angle (SZA), and ozone density at a particular level. The surface albedo used in this calculation is currently fixed to 0.3 for all wavelengths. Some allowance is made for spherical geometry by evaluation of photodissociation rates in the near UV and visible up to SZA $< 96°$. The radiative transfer model used for calculating the rates is a pseudospherical numerical model accurate for SZAs in the range 0°–92°, less accurate for larger SZAs, and covering the wavelength range 120 to 850 nm. Intercomparisons with other models show close agreement for selected species. Cross section and quantum yield data from *DeMore et al.* [1997] are used where available. We have also incorporated the details of the long wavelength tail [*Talukdar et al.,* 1998; *Ravishankara et al.,* 1998] for $O(^1D)$ production from O_3 photolysis. For O_2 photolysis in the Schumann-Runge Bands (SRB) from 175 to 202 nm, the parameterization of *Koppers and Murtagh* [1996] has been used. The radiative transfer code itself is based on the matrix operator doubling and adding scheme described by *Plass et al.* [1973], and more details are given by E. Griffioen and L. Oikarinen (LIMBTRAN: a pseudo three-dimensional radiative model for the limb–viewing imager OSIRIS on the ODIN satellite, submitted to Journal of Geophysical Research, 1999).

The original chemical module did not have aerosol or polar stratospheric cloud (PSC) chemistry. The results presented here still lack PSC chemistry, but in the lower stratosphere a background aerosol climatology [*WMO,* 1995] has been added to allow the incorporation of two important hydrolysis reactions that occur on sulphate aerosols:

$$N_2O_5 + H_2O(a) \rightarrow 2HNO_3$$
$$BrONO_2 + H_2O(a) \rightarrow HOBr + HNO_3.$$

These reactions act to convert active odd–nitrogen into less reactive nitric acid and also result in an important additional source of HO_x via the breakdown of H_2O [*Lary et al.,* 1996]. It is well known that the aerosol distribution in the stratosphere has not been constant over the last 20 years [*WMO,* 1999, chap. 3], with changes driven by major volcanic eruptions such as Mount Agung and Mount Pinatubo as well as many other smaller eruptions that have penetrated the stratosphere. However, since we are attempting to calculate a climatology, we have adopted the baseline mean average aerosol distribution from *WMO* [1992, chap. 8].

3. Model Results

For the results described herein, the model has been run in an interactive mode by which it is meant that the ozone and water from the chemical module are used to

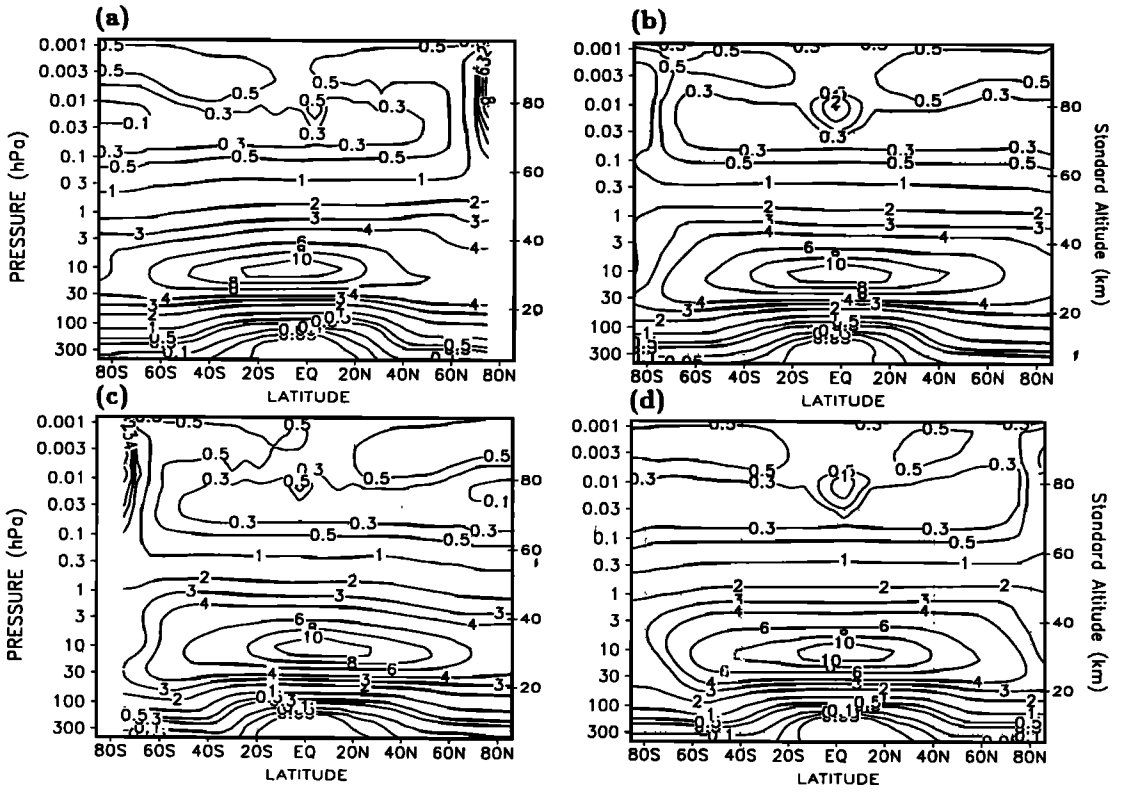

Figure 1. Zonal and monthly mean daytime ozone mixing ratio (in ppmv) averaged over 10 years: (a) January, (b) April, (c) July, and (d) October.

calculate the solar and IR heating which in turn modify the dynamics (transport and temperatures). Long-lived species were initialized using the two-dimensional model climatology from *Brasseur et al.* [1990]. The model was run for 33 years, including a 23–year spin–up period during which several changes were made to the model. For example, reactions on sulphate aerosol were implemented after 13 years of integration. Comparison with the earlier results shows only a small impact on the model climate but with the expected changes in the species partitioning. An analysis of the results from the last 10 years of the simulation is presented below.

3.1. Monthly Mean Distribution

The four panels in Figure 1 show the model 10–year zonal and monthly mean daytime ozone distribution for January, April, July, and October. The daytime values have been presented since there is a diurnal variation in ozone forced by photochemistry above ~1 hPa which becomes quite large in the upper mesosphere [*Brasseur and Solomon,* 1984]. The figure shows the main characteristics of the observed ozone climatology with a maximum of 11 ppmv near 10 hPa at the tropics and with a seasonal variation in the latitudinal position of the ozone peak that follows the direction of the overhead Sun. In the lower stratosphere, ozone isopleths tilt downward from the equator to the pole due to transport by the Brewer–Dobson circulation. This effect is more pronounced in the winter hemisphere because of the increase in ozone photochemical lifetime together with enhanced transport by planetary waves. In the upper stratosphere, ozone isopleths tilt upward toward the winter hemisphere with higher values associated with regions of colder temperatures. Throughout the mesosphere the ozone decreases with height, while in the mesopause region a secondary maximum is evident which is due principally to the ozone production through O_2 photolysis in the Schumann–Runge continuum and to the downward transport of atomic oxygen from the thermosphere.

To compare with observations, we have used the COSPAR International Reference Atmosphere (CIRA) ozone reference model [*Keating et al.,* 1990]. Figure 2 assesses the CMAM performance throughout the entire middle atmosphere domain by presenting the ratio of CMAM ozone mixing ratio to the reference model for January and July. The magnitude of the discrepancy between the model and measurements reaches 20% in the upper stratosphere near the equator. Part of this effect can be attributed to the fact that the chlorine background adopted in this study is about 3.5 ppbv which is significantly larger than the early 1980s values corresponding to the time of the measurements used in the CIRA compilation. Off–line calculations indicate that the model ozone would likely increase by 10% in the upper stratosphere if chlorine levels were more consistent

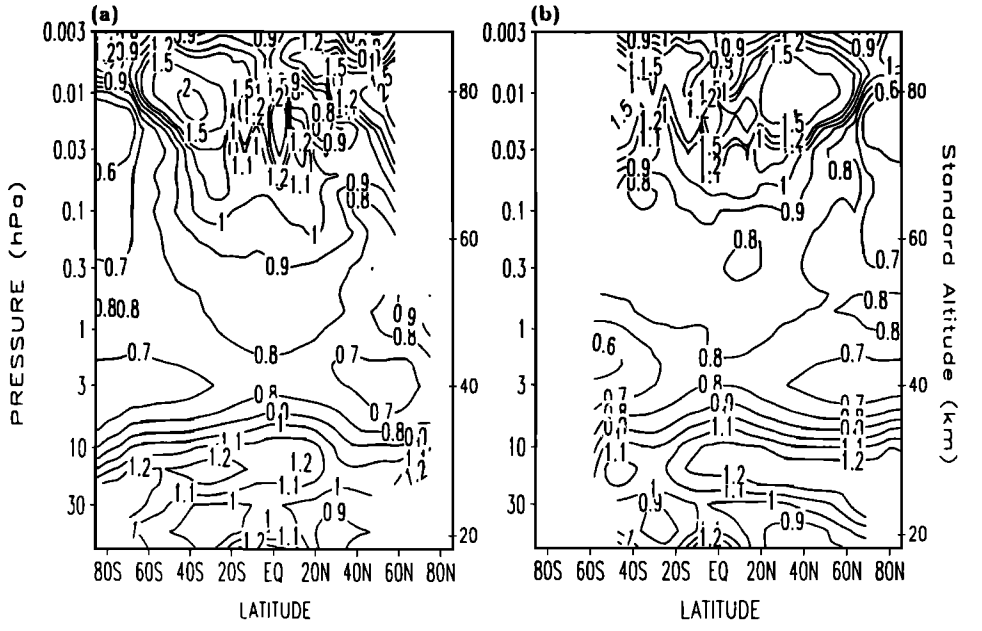

Figure 2. Ratio of model 10-year mean daytime ozone to CIRA [*Keating et al.,* 1990] for (a) January and (b) July.

with the early 1980s values. Another significant factor is the ozone variation caused by the 11 year solar cycle which is not included in the calculation of photolysis rates. We estimate that a few percents of the discrepancies at 40 km could be associated with the fact that the CIRA compilation was taken during maximum solar activity [see *McCormack and Hood*, 1996]

Other important factors such as the transport of ozone precursors from the surface to the upper stratosphere also need to be addressed. It is clear that the closure of the ozone budget relies on accurate estimation of various constituents such as ClO and NO_2 [*Dessler et al.*, 1996] and BrO. In the CMAM as in other models [*Hall et al.*, 1999] the transport of nitrous oxide, CFCs, and other trace species from the troposphere and within the stratosphere is generally too rapid, and this will have a direct impact on the distribution of these key short–lived constituents. Furthermore, the photochemical module does not include all the latest improvements in terms of photochemical rates which have been introduced in various models to produce a better closure of the photochemical ozone budget [*WMO,* 1999, chap. 6]. This latter question remains to be addressed, although some sensitivity tests have indicated that this model generally responds weakly to such changes in the photochemical rates. Finally, the use of one single data set for comparison is somewhat misleading. Indeed, comparison with Upper Atmosphere Research Satellite (UARS) data [*Croteau,* 1998] shows discrepancies of the order of 20% throughout the upper stratosphere, suggesting that there may also be inconsistencies (due to calibration for example) between the CIRA and Microwave Limb Sounder (MLS) data sets. Clearly, these different factors need to be isolated before being able to fully explain the reasons for such discrepancies in the region. On another aspect the figure also shows the model deficiency in representing the upward tilting of ozone isopleths at high latitude. Further experiments at higher resolution are planned to try to address this problem by improving the transport of ozone and its precursors.

Between 10 and 20 hPa, Figure 2 suggests that the model overestimates the ozone mixing ratio by more than 20%. A few percent of this discrepancy can be attributed to the model ozone underestimation occurring above, which allows more radiation to penetrate into the lower stratosphere, thereby producing more ozone in the region where photochemistry is less active in removing it. However, our analysis indicates that the ozone transport in this region is difficult to represent accurately due to the combined effect of a low model resolution and the presence of a strong ozone gradient. As it is, however, the sizeable disrepancies between CMAM and CIRA are restricted to a limited region and have little impact on the overall integrated quantities such as column ozone.

In the upper mesosphere and mesopause regions the model bias appears relatively large. In this region the ozone distribution is driven by the photochemistry and the transport of atomic oxygen. The large model dynamical variability in the region and the proximity of the species boundary conditions both contribute to produce large uncertainties in the results. The CIRA climatology itself indicates substantial uncertainty in the ozone data throughout most of the region due to the limited number of measurements used in the compilation. Given this level of uncertainty in both model and observations, and the large amount of variability in the

model data (see Figure 11 below), the large ratios seen above 0.05 hPa do not have the same significance as those seen below.

3.2. Troposphere and Lower Stratosphere

Figure 3 shows the July ozone density from the surface to 10 hPa. In this region, ozone can be considered as a long–lived species (outside regions of regional air pollution and biomass burning, etc., as discussed by *Müller and Brasseur* [1995]), and hence its distribution can provide a useful assessment of the model transport. The figure shows that in the troposphere, ozone is flowing to the surface sink with characteristic number densities of $\sim 5 \times 10^{11}$ molecules cm^{-3}. The values are a little higher in the Northern than in the Southern Hemisphere, which appears to be consistent with the greater mass flux from the stratosphere to the troposphere in the NH [*Rosenlof and Holton*, 1993; *Holton et al.*, 1995]. The figure also shows that the ascent in the tropics creates a region of low ozone in the free troposphere with characteristic values below $\sim 5 \times 10^{11}$ molecules cm^{-3}.

The tropopause, which delineates the different mixing properties of the tropospheric and stratospheric reservoirs, is well highlighted by the ozone distribution. The figure clearly shows the transition zone between the vertically stratified lower stratosphere, where ozone gradients are very sharp, and the troposphere within which ozone is relatively well mixed. This "chemical tropopause", as illustrated by the mixing properties of ozone, is located near 100 hPa at the tropics and 400 hPa at high latitudes. The model also reproduces the winter maximum in ozone number density of 6×10^{12} molecules cm^{-3} near 70 hPa and 60°S. This feature reflects the vortex–edge barrier associated with the SH polar night vortex, and is consistent with climatology [*Warneck*, 1988]. Figure 4 shows the seasonal variation of the zonally averaged vertical profile of ozone at 58°N through the last year of the model integration. The downward transport from the stratosphere to troposphere clearly reaches a maximum in late spring and has a minimum in late summer, consistent with the waxing and waning of the Brewer–Dobson circulation [*Appenzeller et al.*, 1996]. In the middle troposphere the signal shows a lag in time by a few weeks as a result of transport.

3.3. Middle and Upper Stratosphere

Figure 5 compares the time series at 10 hPa of the ozone deviation from the annual means for model and observation. In both cases, ozone monthly mean values are used for the individual datapoints making up for the time series. The 3–year model time series (Figure 5a) is compared with the same diagnostic calculated from the single year CIRA data set (Figure 5b). The first panel shows that in the tropics, the model ozone exhibits a semiannual variation with a maximum at the equinox and a minimum at solstice. This signal in the model is driven largely by the variation in photolysis rates with maximum ozone production when the Sun is directly overhead [*Perliski and London*, 1989]. Over the tropics the amplitude of the signal (~3%) is about a factor of 2 smaller than in CIRA. Part of this lack of ozone variability may be caused by the lack of a model quasi–biennial oscillation (QBO), which clearly plays a role in the distribution of long–lived constituents in this region [*Randel et al.*, 1998].

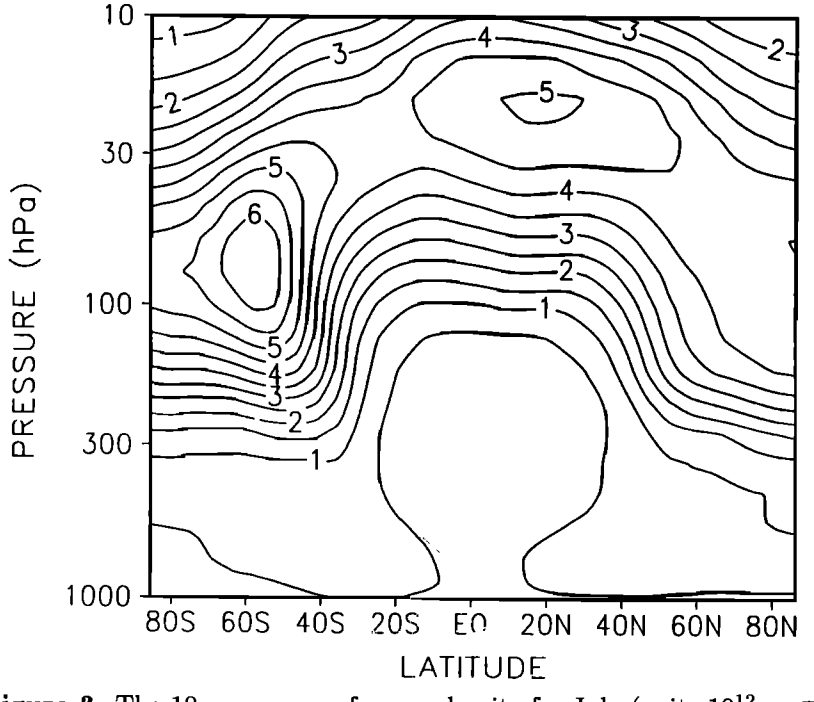

Figure 3. The 10-year mean of ozone density for July (units 10^{12} cm^{-3}).

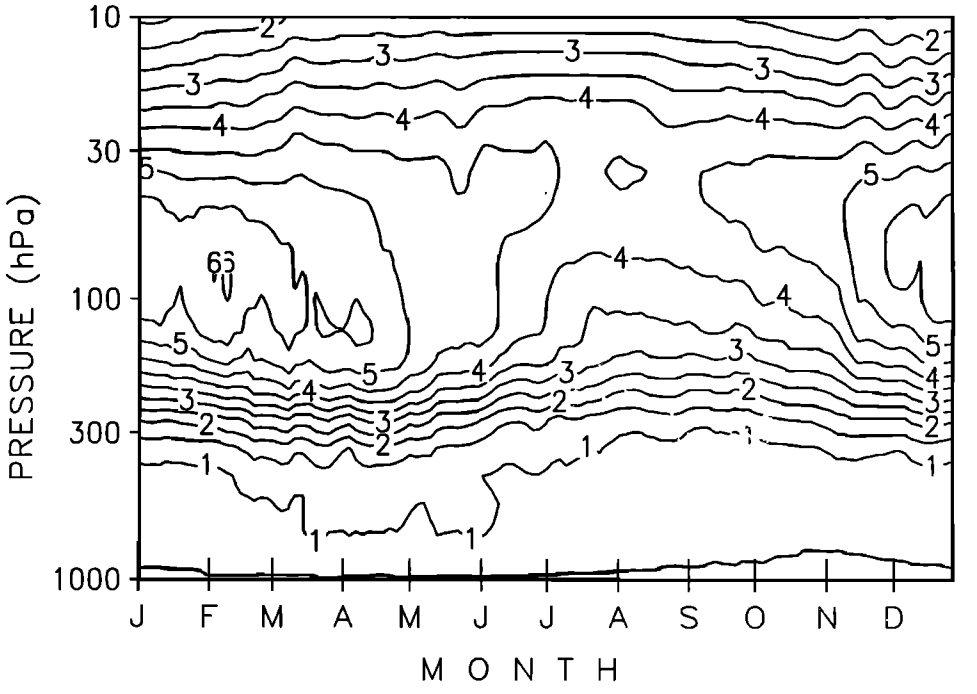

Figure 4. Time series of the zonally averaged ozone cross section (10^{12} cm^{-3}) at 58°N throughout the last year of the model integration.

Outside the tropics the signal becomes annually varying with an amplitude that increases poleward and generally reaches ~15% in midlatitudes, with the extrema occurring close to solstice, in general agreement with the observations. The annual variation becomes larger at higher latitudes since the photochemical ozone sources and sinks are weaker and thus transport plays a much larger role. The spring buildup is followed by a slow summertime decay occurring under the influence of photochemistry. The particularly strong seasonal cycle at 60°S highlights the virtual absence of ozone transport across the vortex edge throughout the winter, followed by the strong intrusion associated with the springtime breakdown of the polar vortex. During winter solstice there are enhanced meridional gradients around 20° with relatively weak gradients in midlatitudes, consistent with the presence of a stratospheric surf zone. A large fraction of the model ozone variability seen outside the tropics is due to the seasonality in the transport of ozone–rich air from the tropics into higher lati-

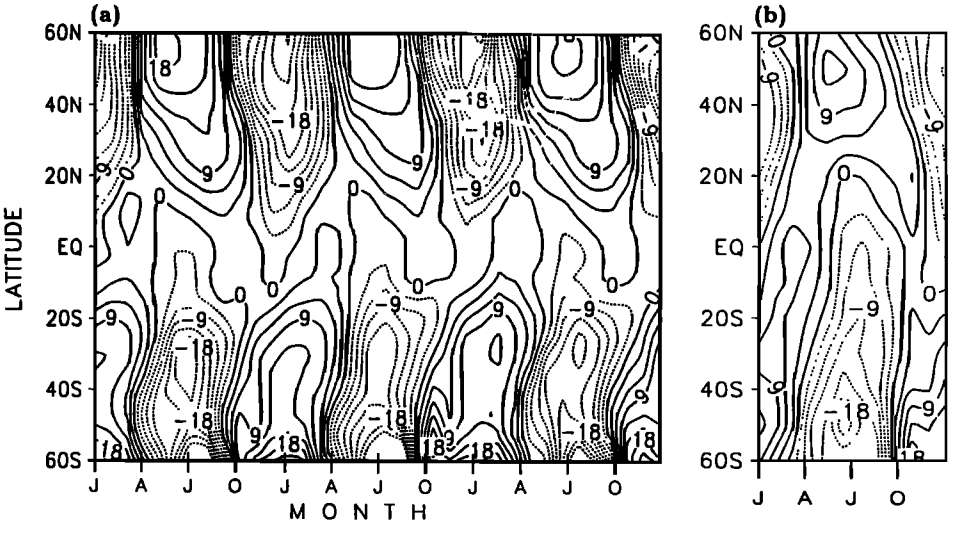

Figure 5. Time series of ozone deviation from the annual means (in %) at 10 hPa. The calculation of the deviation use ozone monthly mean values as individual datapoints, and the means are calculated over the full time length of the data sets: (a) 3 years of model results and (b) single year of CIRA observation.

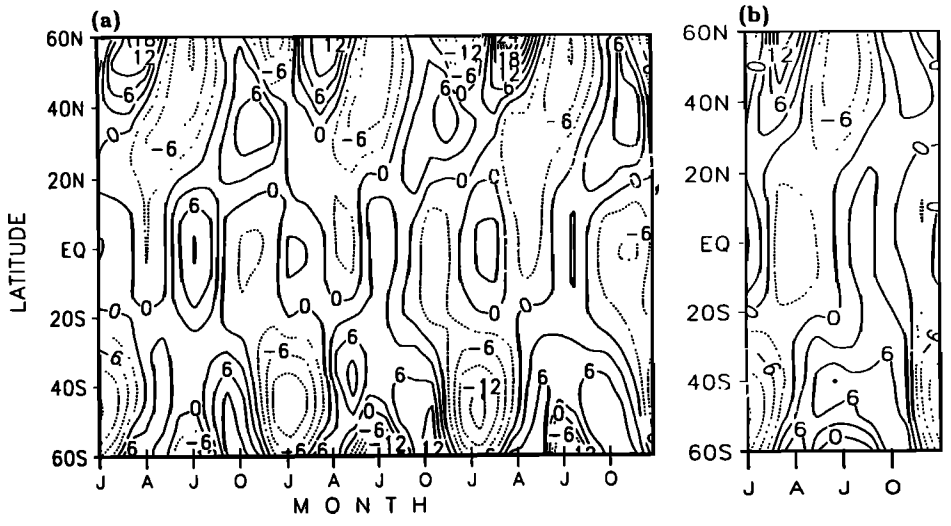

Figure 6. As in Figure 5, but at 3 hPa.

tudes. This effect is likely enhanced by the difficulty of representing sufficiently robust subtropical barriers in coarse–resolution models.

At 3 hPa (Figure 6) the seasonal cycle in the tropics is no longer in phase with the Sun, and the maxima and minima are significantly shifted in time compared with 10 hPa. The fact that the ozone density is out of phase with the solar forcing is due to the impact of the temperature variations. The reaction $O + O_3 \rightarrow 2O_2$, k_o, represents a large fraction of the ozone sink at these heights, and it is very temperature–sensitive. Thus an increase in the temperature at equinox acts to increase the ozone sink via an increase in the rate (cm^{-3} s^{-1}) for the reaction k_o, which counteracts the production maximum at equinox. The increase in the reaction's significance is due both to an increase in the rate constant and to an increase in O density since, as temperature increases, the rate constant for $O + O_2 + M \rightarrow O_3 + M$ decreases. The pattern generated by the model is in good agreement with the measurements, with a nominal amplitude of the variation for both of ~4%.

At midlatitudes, photolysis, temperature, and transport are all important in driving ozone changes. Thus at ~50°at summer solstice, model ozone at 3 hPa is actually a minimum in spite of 24–hour production [see, e.g., *de Grandpré et al.*, 1997, Figure 13]. This is a result of decreased transport from the tropics and increased temperatures, the latter leading to the increase of important loss processes as discussed above. This behavior is in reasonable accord with the measurements in terms of magnitude. We note that the model exhibits a semiannual variation at this latitude in both hemispheres. The measurements, however, only show such a semiannual variation in the NH, whereas the SH exhibits an annual variation with a plateau in ozone from May to September. Meridional transport from the tropics to higher latitudes occurs with varying strength throughout the year. Maximum mixing ratios occur in the NH at latitudes ≥60° during the late–winter/spring when the ozone photochemical lifetime is longest: this suggests that meridional transport at 3 hPa is most rapid at this time of year. In the Southern Hemisphere, maximum mixing ratios also occur in late–winter/spring around 50°–60°S, but the strong polar vortex prevents meridional transport across its edge, as at 10 hPa.

Figure 7 shows the zonal average cross section of the ozone standard deviation from the 10–year mean for the model and compares it with the CIRA climatology. The results indicate that both the upper stratosphere and lower stratosphere have large variability throughout the year. The two model maxima in the ozone variability at 50°N and 50°S and ~1.5 hPa are located close to those of the observations although they are less intense by a factor of 2 to 3. This mostly highlights the fact that the model is unable to produce sufficient upward tilt of the ozone isopleth in the winter higher latitudes. We note that this model deficiency is not very temperature–dependent since more recent integrations with a significantly cooler upper stratosphere show the same effect. In the lower stratosphere the enhanced seasonal variability seen in the model below 10 hPa is likely driven by an enhanced model transport as compared with observations. The location of the maximum variability at 45°N is in general agreement with observations, whereas the 35°S maximum appears to be shifted due to the strength of the SH polar vortex in the model, which moves the mixing barrier toward lower latitudes throughout most of the year.

3.4. Mesosphere

The current version of the model includes a reaction set adequate to represent the ozone behavior throughout the mesosphere and lower thermosphere. In the mesosphere the ozone photochemistry is, in some respects, simpler than in the stratosphere due to the re-

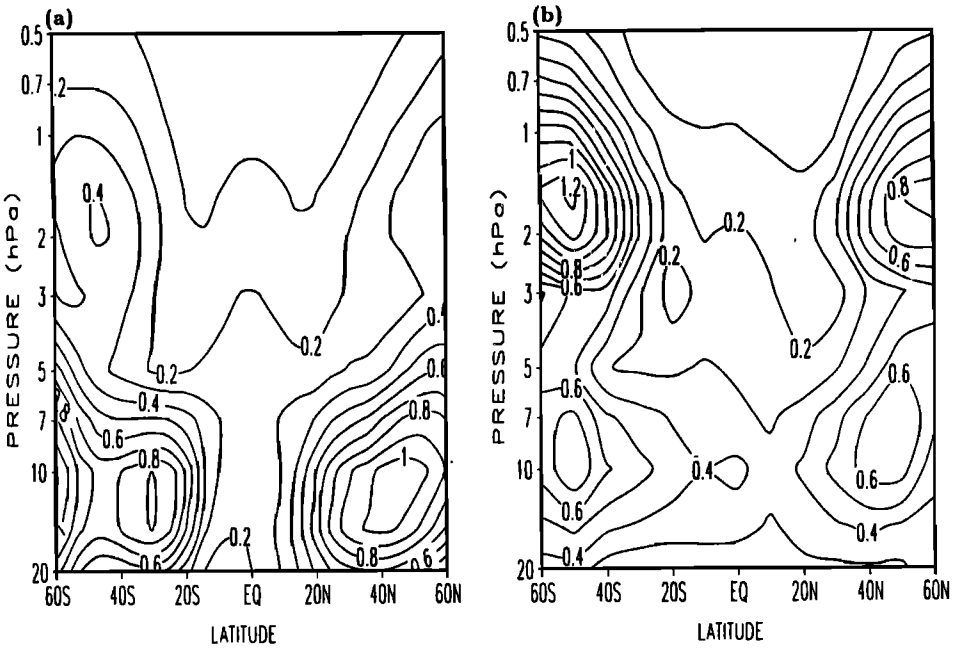

Figure 7. Zonal average cross section of ozone standard deviation from the annual mean (in ppmv). The calculation of the deviation uses ozone monthly mean values as individual datapoints, and the mean values are calculated over the full time length of the data sets: (a) 10 years of model results and (b) single year of CIRA observation.

duced importance of odd-nitrogen and halogens in the odd-oxygen budget. Above about 60 km, atomic oxygen becomes the major form of O_x since ozone production from the 3-body reaction, $O + O_2 + M \rightarrow O_3 + M$, falls off rapidly with height. Also, since ozone is photolyzed rapidly during the day, it has a distinct diurnal signature in the mesosphere and above. The source of O_x in the mesosphere is largely the photolysis of O_2 in the Schumann–Runge bands, whereas in the overlying lower thermosphere, photolysis in the Schumann–Runge continuum and transport of O from the thermosphere are also important processes. Figure 8 shows for March conditions and low latitude the ozone time series at several pressure levels taken from a special run where the data were stored every hour. The results show a progressive decrease of ozone with altitude and a clear increase with altitude of the amplitude of the diurnal variation. The smooth transitions seen at sunrise/sunset illustrate the overall stability of the numerical solver at various heights. The results are in reasonable agreement

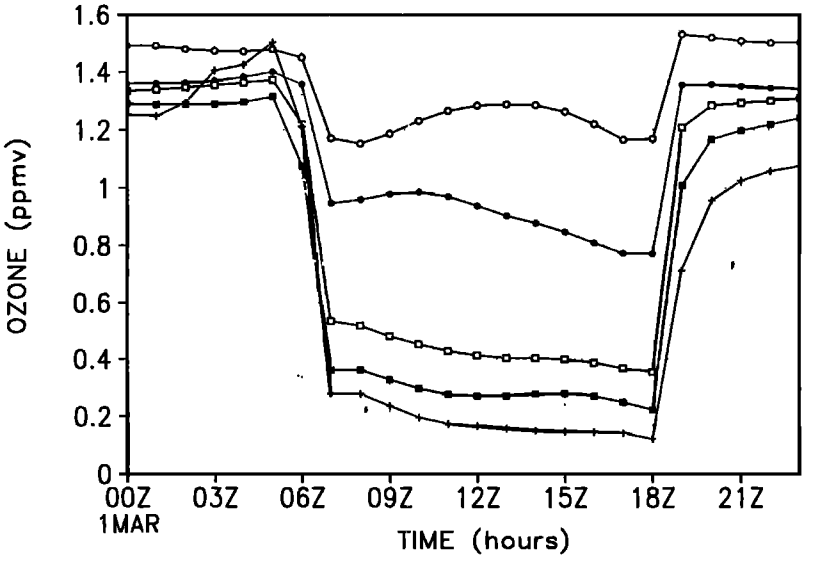

Figure 8. Diurnal variation of model ozone for March 1 at the equator: Open circles, 0.3 hPa., closed circles, 0.2 hPa., open squares, 0.1 hPa., closed squares, 0.07 hPa., and crosses, 0.05 hPa.

with the ozone diurnal behavior as measured from the ground using millimeter wavelength instruments [e.g., *Kawabata et al.*, 1997; *Sandor and Clancy*, 1998, and references therein].

For this version of the CMAM, unusually high values of O_3 occur in the upper mesosphere polar night (some hint of this feature can be seen in Figure 1). These high ozone values result from the inadequate representation of the HO_x chemistry in the polar night since HO_x is not transported in the model and so the main sink of ozone, $H+O_3 \rightarrow OH+O_2$, shuts off with the setting of the Sun. Preliminary results have indicated that better agreement with observations can be obtained by improving the representation of HO_x constituents via their transport. In the current model the radiative impact of this effect is negligible since it mainly occurs in the polar night. Nevertheless, with the incorporation of chemical heating, the potential impact of such features is potentially important and will need to be addressed.

3.5. Ozone Column

Figure 9a shows the 10–year average column ozone time series, Figure 9b shows CIRA climatology, and Figure 9c shows the ratio of the two quantities. It is seen that the magnitude and phase of the seasonal variations are generally well represented by the model in most regions. Over the tropics the agreement with observations is within 5% which suggests a good performance by the photochemistry and dynamics.

The model also reproduces the phase and magnitude of the equinox maximum and minimum at mid and high latitudes in both hemispheres. It reproduces with some

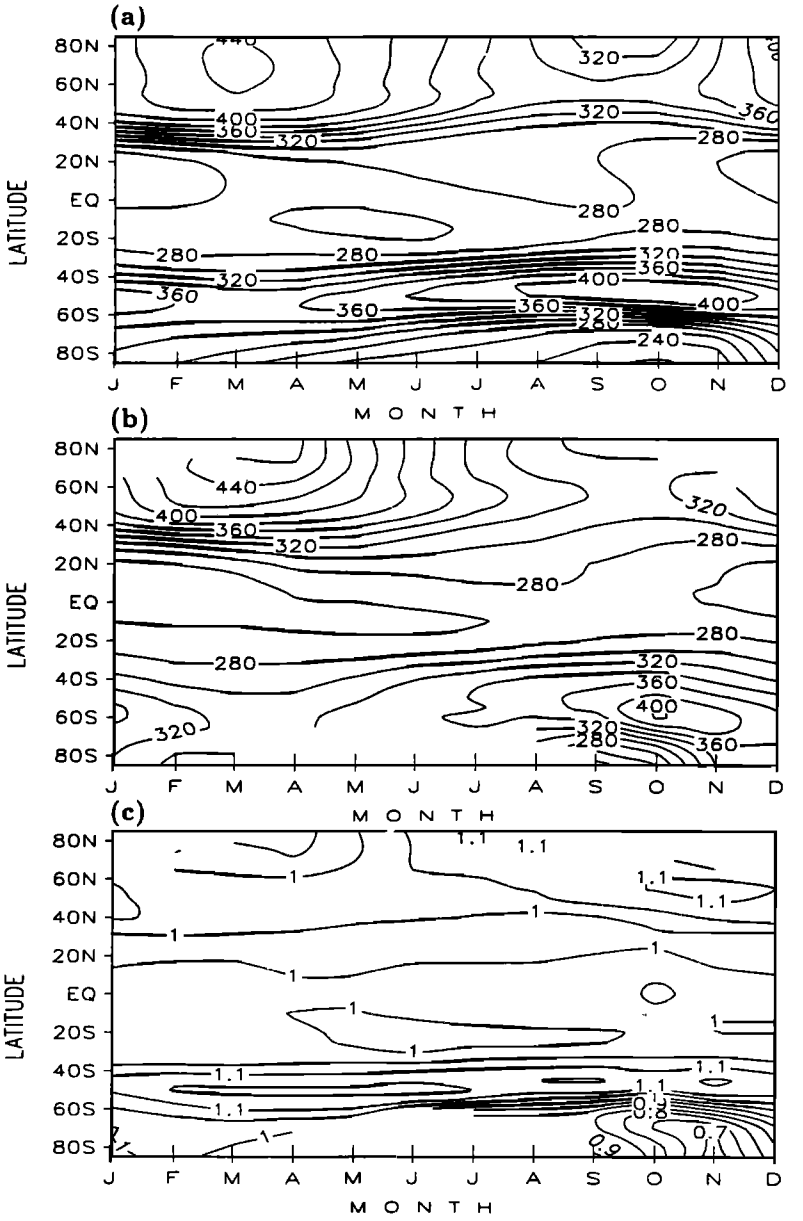

Figure 9. Annual cycle (latitude versus time) of column ozone (DU): (a) 10-year mean of model, (b) CIRA, and (c) model over CIRA.

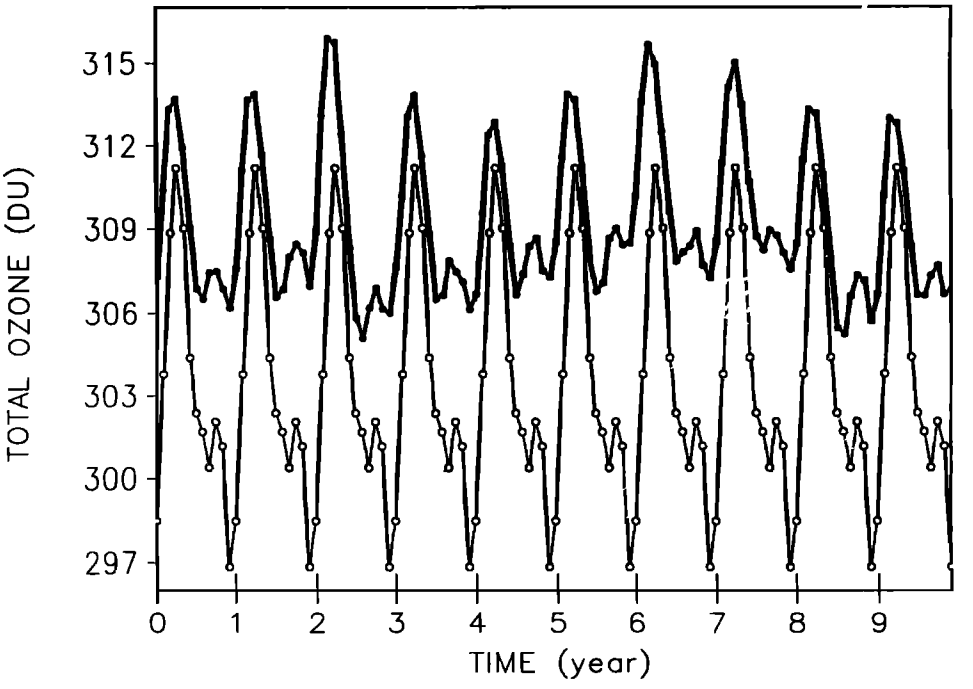

Figure 10. The 10-year time series of globally averaged column ozone (DU). The thick line is model results, and the thin line is the single-year CIRA data set repeated over 10 years.

realism the seasonal evolution of the SH polar vortex, represented by the progressive buildup of the vortex throughout the year and the late spring breakup. Minimum column ozone reaches 220 Dobson units (DU) in October, a value which is significantly lower than what is expected from pre-ozone hole conditions [*Cariolle et al.*, 1990; *WMO*, 1999, chap. 4]. The strong Antarctic ozone minimum in this version of the CMAM is a transport-induced minimum, reflecting a systematic dynamical bias in the climatology: the Antarctic vortex breaks up too late in the year, which implies too little descent while at the same time preventing meridional transport into the polar region. This demonstrates the impact of dynamical biases on the ozone distribution, something that needs to be adequately investigated before implementation of more complex processes such as heterogeneous chemistry.

Figure 10 shows the globally averaged column ozone over 10 years of the model compared to the CIRA ozone (the latter being repeated for each year). The results show that model ozone is well conserved on a decadal timescale and is overestimated by roughly 3% compared with CIRA throughout the full period. Both the CIRA and model total ozone exhibit two peaks in their annual cycles with the October peak being the weakest. These maxima occur when the mid to high latitude ozone column amounts are peaking, a phenomenon that occurs in spring but is much stronger in the NH than in the SH spring. This is the result of stronger planetary wave activity, leading to greater transport of ozone, in the NH as compared with the SH winter. The discrepancies between the model and CIRA are more accentuated toward the end of the year so that the October peak is higher and the amplitude of the annual cycle is smaller. This is partly due to the excess amount of ozone modeled in SH midlatitudes; it persists all year but mostly affects the global ozone in the second half of the year when the SH ozone becomes dominant in determining the shape of the total ozone.

3.6. Ozone Variability

An important aspect of MAMs is their capability to provide a comprehensive representation of the ozone spatio-temporal variability at various scales. The panels in Figure 11 show for January, April, July, and October the daytime monthly mean standard deviation calculated using the information stored every 3 days and accumulated over the 10 year period. The ozone variability patterns are generally similar for solstice conditions (Figures 11a and 11c) with low variability values in the summer hemisphere and a progressive increase toward the winter hemisphere. The region of minimum variability covers most of the upper stratosphere and lower mesosphere. In this region the ozone distribution is driven by photochemistry, and the low degree of simulated variability (below 2%) reflects a low degree of variability for the temperature and other constituents. At high latitudes the variability is large and differs noticeably between winter and summer, which is consistent with the dynamical control of ozone in the polar night. In the regions below 50 hPa and above 0.05 hPa,

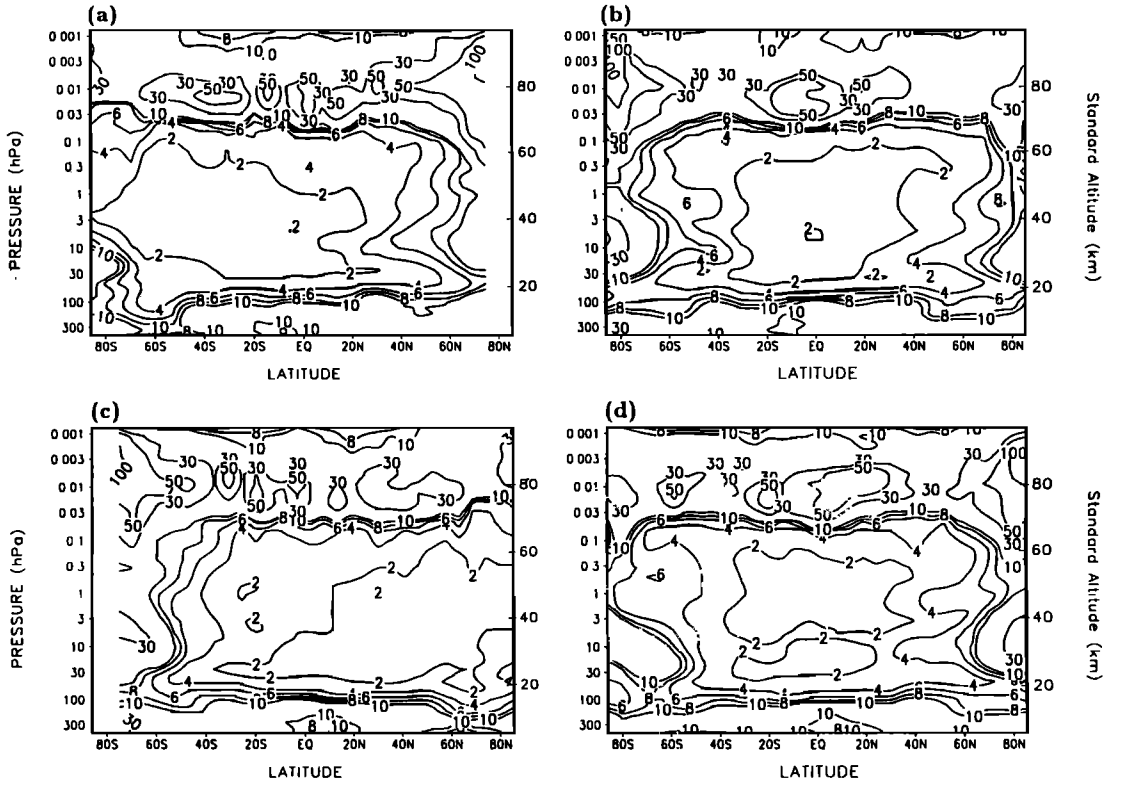

Figure 11. Ozone 10-year monthly mean standard deviation in (in %). The individual datapoints making up the calculation are the 3-days zonal mean values of ozone calculated at every model dumping intervals. The mean is calculated over the full time length of the data sets: (a) January, (b) April, (c) July, and (d) October.

transport generally dominates over photochemistry, and therefore the ozone variability is larger.

Figure 12 shows the ozone variability based on 4 years of measurements from the Solar Backscatter Ultraviolet instrument, taken from *Keating et al.* [1990]. It shows that the model results compare reasonably with observations throughout the various seasons. For solstice conditions the 10% contour in the winter hemispheres occurs around 60°–70° for both the model and the observations. The observed symmetry centered at the equator during equinox is also captured by the model. However, in general, the model appears to produce lower variability than the measurements in the summer hemisphere where ozone is photochemically active. This phenomenon could be attributed to the fact that some of the variability in the region potentially comes from scales that are below the model resolution. The model diffusion may also produce too strong homogenization of ozone and its precursors at resolved scales. In polar regions the effect is reversed, and the model generally shows larger variability than the measurements throughout the year. In this case, the variability can be provided by large–scale features such as planetary waves. Model analyses [*Chaffey,* 2000] indeed indicate that the model exhibits too many northern stratospheric warmings compared to measurements. Nevertheless, further investigation using more extended data sets is required to better characterize this effect. We note finally that an interesting discrepancy between the simulation and observations appears between 20 hPa and 10 hPa. In this region the model predicts a minimum percentage variability throughout the year, whereas the CIRA shows the opposite. This is likely associated with the modeled high ozone bias in this layer (see Figure 2), which lowers the percentage variability.

In the mesopause region, ozone is considerably more variable on a daily basis than it is in the stratosphere. Figure 11 shows that the monthly variability is large in the region and has the same order of magnitude as the model monthly mean biases seen on Figure 2. It shows the necessity of characterizing the ozone variability from measurements in this region to address climatological trends of ozone and other constituents. In the winter mesosphere the high ozone variability appears to come from the downward transport of ozone, as suggested by the downward tilting of the isopleths. Such variability is expected as the model dynamics is largely driven by gravity–wave–induced downwelling in this region.

4. Ozone Radiative Feedback

The results presented so far have included "radiative feedback", namely, the use of prognostic ozone and water vapor to calculate the heating rates. In order to iso-

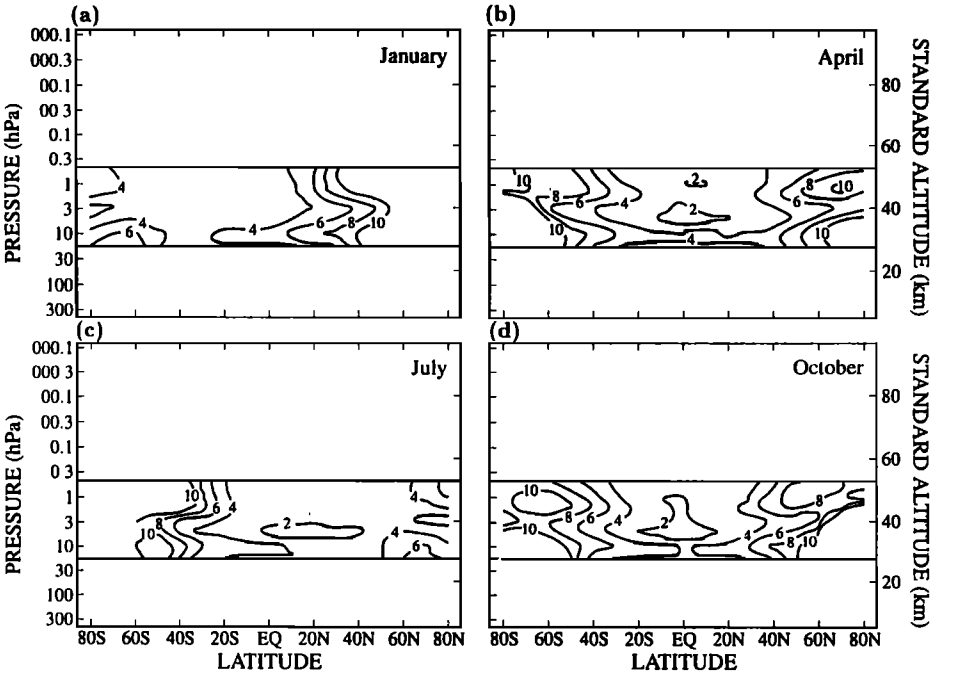

Figure 12. Same as Figure 11, but for 4 years of SBUV results. (Adapted from *Keating et al., 1990*, Figure 6, chap. 15 with permission from the Committee on Space Research).

late the effects of the radiative feedback on the model climatology, CMAM has also been run with no radiative feedback (i.e., using climatological ozone and water for radiative forcing inputs) for 3 years. Although a 3-year simulation may be somewhat short in general for identifying anomalies, it appears adequate in this case given the magnitude of the effects. Figure 13 shows the temperature differences between the model and CIRA climatologies [from *Fleming et al.*, 1990] for January and July for both the noninteractive (Figures 13a and 13b) and interactive case (Figures 13c and 13d). We note that these results were produced with an earlier version of the model which included a GW source different from the one otherwise used in this study. This GW source produced a robust warm temperature anomaly in the winter SH lower stratosphere, forced by the overly strong adiabatic descent within the polar vortex. This model version also tended to generate a cold anomaly in the lower stratosphere, which may be associated with the use of the Morcrette radiation scheme which overestimates cooling in this region [see *Fomichev and Blanchet*, 1995]. However, these systematic model biases are irrelevant to the conclusions drawn below.

In regions where the model is close to radiative equilibrium, the results show that the impact of including interactive ozone in the model is significant. Over the tropics near the stratopause, the interactive run produces cooler temperature by 5 to 8 K compared with the noninteractive results, a radiative effect likely generated by lower simulated ozone compared with the CIRA climatology used in the noninteractive run (compare with Figure 2). The temperature differences between the two runs generally maximize throughout the upper stratosphere/lower mesosphere region but are not uniform. In the summer hemisphere high latitudes the warm anomalies (~12 K) which exist in the control run have been reduced significantly with the use of interactive ozone. In this region it is known that the atmosphere is close to radiative equilibrium and is essentially dependent upon the local amount of ozone. The fact that the model temperatures for the interactive run agree well with CIRA temperatures in the vicinity of the summer stratopause, while the density of O_3 is low compared with CIRA O_3 (Figure 2), suggests a possible inconsistency between the CIRA temperature and ozone climatologies in this region. In the lower mesosphere summer the ozone sink due to the Chapman reactions, which are temperature–dependent, can provide an important negative feedback controlling temperature in an interactive model. However, it is also conceivable that the CIRA temperature and ozone measurements are consistent and that the model's improvement is the result of cancelling errors. More detailed analysis using independent measurements from UARS could clarify some of these uncertainties.

5. Further Discussion and Model Development

For the transport of species the current results show that the spectral technique remains relatively accurate if careful attention is paid to avoid the development of sharp gradients in species distributions. In the current context the use of the family approach for the transport

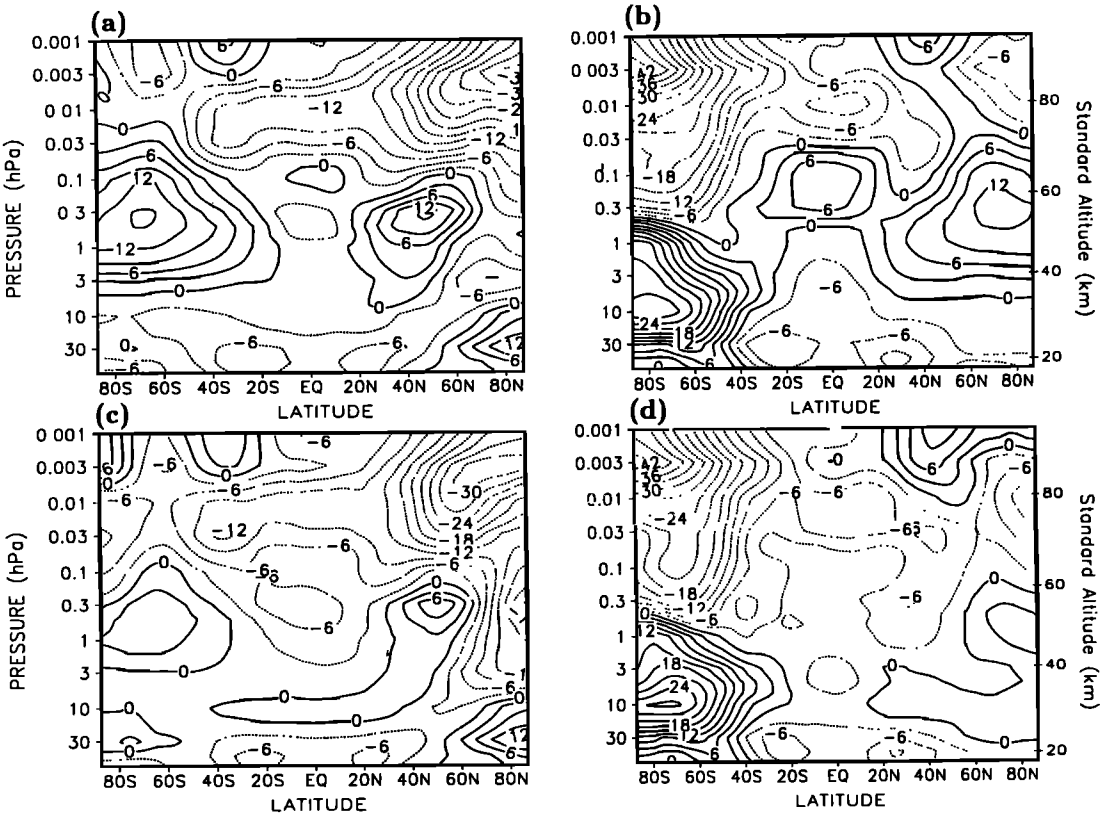

Figure 13. The 3-year monthly mean temperature difference (K) between model and CIRA [*Fleming et al.*, 1990]. With noninteractive chemistry for (a) January and (b) July, and with interactive chemistry for (c) January and (d) July.

of short–lived constituents was necessary and, evidently, largely sufficient to prevent any numerical problems associated with the hole–filling scheme. The results show in particular that the global conservation of all constituents and families is well modeled without having to explicitly incorporate any artificial mass conservation measures. Given the length of the model integrations and the need to study long–term trends, this property of the spectral technique is very important. The spectral technique also preserves quite well the large–scale gradients in species distributions, which is an important requirement in the middle atmosphere where gradients are sometimes large and can persist for several months. The method is also relatively inexpensive in terms of CPU and memory requirements, and is numerically stable. However, with the future implementation of heterogeneous chemistry and thus the potential for additional processes occurring in very limited areas, the use of spectral transport becomes problematical due to its inability to properly represent small–scale features. Other transport scheme alternatives are being investigated.

On the aspect of the ozone deficit, there has been much recent work that applies to this problem [*WMO*, 1999, chap.6]. Building on earlier work, *Khosravi et al.* [1998] addressed the ozone deficit problem in the upper stratosphere below about 50 km and found that much of the problem revolves around the rate for $O + HO_2 \rightarrow OH + O_2$, which they suggest should be about 40% lower than listed in the Jet Propulsion Laboratory (JPL) compilation [*DeMore et al.*, 1994, 1997]. They also suggest that HCl production from $OH + ClO \rightarrow HCl + O_2$ plays an important role. Above, in the mesosphere, contemporaneous (or nearly so) measurements of OH, HO_2, H_2O, and O_3 by several groups along with modeling studies also implicate the $O + HO_2 \rightarrow OH + O_2$ rate constant [*e.g., Jucks et al.*, 1998; *Summers et al.*, 1997; *Sandor and Clancy*, 1998]. The results among the different groups are not consistent, but they do clearly point to the need for more laboratory work on the above reaction, as well as on $O + OH \rightarrow H + O_2$ and $OH + HO_2 \rightarrow H_2O + O_2$, before further assessment is made of their implementation in any model used for climate simulations. The importance of the possibility of acid production from the $OH+ClO \rightarrow HCl+O_2$ reaction appears to have been first suggested by *McElroy and Salawitch* [1989], and its importance has been alluded to above. We have included this reaction and a similar one for HBr production using the work of *Chartrand and McConnell* [1998] as a guide for the rate constants, and have performed some sensitivity tests in the CMAM with and without these rates. We have found only mod-

est increases in ozone of the order of 3–4% in limited areas with the inclusion of these rates and the use of the model's prognostic CH_4. These findings are similar to those of *Khosravi et al.* [1998], who point out that there is better agreement when CH_4 observations as opposed to model CH_4 values are used.

An important missing element necessary for long–term simulations, particularly those which aim to investigate the possibility of the development of a boreal ozone hole [*Shindell et al.*, 1998], is polar stratospheric cloud (PSC) chemistry. The heterogeneous chemistry module is currently being tested on–line and should be available for long–term integration in the near future. The utility of simulations with PSCs will also depend on the model's capability to reproduce a reliable winter–spring climatology in the polar regions, most notably the strength and stability of the polar vortices and their transient evolution. In this respect, an improved understanding of the most appropriate GW source distributions for GWD parameterization schemes is required. Another important aspect of Arctic polar dynamics to be investigated is the frequency and strength of sudden stratospheric warmings for which models generally differ from observations [*Pawson et al.*, 2000].

Sensitivity studies are also planned to improve the vertical resolution of the model in the region covering the upper troposphere and lower stratosphere. The tropical tropopause region is known to be important for transport between the troposphere and stratosphere, with this region playing an important role in the budget of long–lived constituents. Accurate simulation of the transport processes in this region is therefore particularly important. High vertical resolution in this region could potentially be very beneficial in the model, helping to improve the distribution of temperature and water vapor, and hence allow us to address climate issues related to ozone trends and aircraft emissions. Such new applications would also require further model development in the upper troposphere, for example, including the downward extension of the chemistry module and the implementation of a database of emissions of ozone precursors.

The calculation of photolytic rates and radiative heating rates are two independent calculations in this version of the model, and there are definite plans to make both calculations consistent in a future version of the model. This work would require significant changes to the shortwave radiation code such as adding new spectral intervals and calculating solar heating over narrower spectral intervals. The mesosphere and lower thermosphere regions are areas where further model developments are also necessary to include chemical heating processes which can potentially play an important role in the energy budget [*Mlynczak and Solomon*, 1993]. Work is also underway aimed at investigating the need to raise the lid of the model to improve dynamics in the mesosphere and lower thermosphere [*Beagley et al.*, 2000]. These developments could have an impact that propagates down and potentially improves the model climatology and species distribution over the entire model domain.

6. Summary

The Canadian Middle Atmosphere Model has been used to study the ozone distribution throughout a domain that extends from the surface to approximately 95 km. The model is radiatively coupled with an on–line photochemical module that provides prognostic ozone and water vapor at every time step from the middle troposphere to the top of the model. First–order diagnostics from a 10–year model integration have been compared with the CIRA climatology. In the stratosphere the results are in general agreement with the reference model in terms of monthly mean and seasonal variability. The main area of discrepancy with the observations is in the upper stratosphere, where the model appears to underestimate ozone background conditions.

The model conserves important quantities such as total ozone and column ozone over a long timescale. The results showing interannual and seasonal evolution of column ozone also indicate that the general circulation and ozone budget are well reproduced. The model also provides a comprehensive representation of ozone monthly mean variability for solstice and equinox conditions. The results show furthermore that the model is capable of representing processes over a large domain and a wide range of timescales, from large diurnal variations in the mesosphere to the seasonal cycle in stratosphere–troposphere exchange.

The impact of incorporating ozone radiative feedback on the model climatology has been analyzed. The results show that minor changes in the ozone distribution may have a significant impact upon model temperatures in specific regions, particularly in the summer stratopause region where the atmosphere is near radiative equilibrium. In the case of CMAM the incorporation of the ozone radiative coupling has removed a persistent warm bias in the model and brought the CMAM temperatures closer to CIRA despite the fact that modeled ozone is lower than the CIRA climatogical values. This result raises some questions about a possible inconsistency between the two CIRA data sets. The study shows that the CMAM with interactive ozone can be used in a large range of applications which require the inclusion of a comprehensive representation of photochemical feedbacks.

Acknowledgments. The MAM project involves colleagues from the University of Toronto, York University, Université du Québec à Montréal, Dalhousie University, the Canadian Centre for Climate Modelling and Analysis (CCCma) of the Meteorological Service of Canada (MSC) (formerly the Atmospheric Environment Service), and the Centre for Research in Earth and Space Technology (CRESTech). Our thanks go to all those involved in working with the CMAM at CCCma and the atmospheric modeling group at York University for their assistance. We are grateful to

Andreas Jonsson of the University of Stockholm and Jason Chaffey and John Fyfe of the University of Victoria and CCCma for communication of their results. We would like to thank the two anonymous reviewers for helpful insight and comments. J. McConnell also wishes to thank Keith Ryan and Ian Plumb of CSIRO, Lindfield, for hospitality and useful discussions while on sabbatical at CSIRO. This work was funded by the Natural Sciences and Engineering Research Council of Canada, and by the MSC through its Climate Research Network.

References

Abdella, K., and N. A. McFarlane, Parameterization of the surface-layer exchange coefficients for atmospheric models, *Boundary-Layer Meteorol., 80,* 223-248, 1996.

Appenzeller, C., J. R. Holton, and K. H. Rosenlof, Seasonal variation of mass transport across the tropopause, *J. Geophys. Res., 101,* 15,071-15,078, 1996.

Beagley, S. R., J. de Grandpré, J. N. Koshyk, N. A. McFarlane, and T. G. Shepherd, Radiative-dynamical climatology of the first-generation Canadian Middle Atmosphere Model, *Atmos. Ocean, 35,* 293-331, 1997.

Beagley, S. R., C. McLandress, V. I. Fomichev, and W. E. Ward, The extended Canadian middle atmosphere model, *Geophys. Res. Lett.*, 27, 2529-2532, 2000.

Brasseur, G., and S. Solomon, *Aeronomy of the Middle Atmosphere*, 441 pp., D. Reidel, Norwell, Mass., 1984.

Brasseur, G., M. H. Hitchman, S. Walters, M. Dymek, E. Falise, and M. Pirre, An interactive chemical dynamical radiative two-dimensional model of the middle atmosphere, *J. Geophys. Res., 95,* 5639-5655, 1990.

Cariolle, D., A. Lasserre-Bigorry, J.-F. Royer, and J.-F. Geleyn, A general circulation model simulation of the springtime Antartic ozone decrease and its impact on midlatitudes, *J. Geophys. Res., 95,* 1883-1898, 1990.

Chaffey, J., Arctic polar vortex variability in the Canadian middle atmosphere model, M.Sc. thesis, Univ. of Victoria, Victoria, B.C., Canada, 2000.

Chartrand, D. J., and J. C. McConnell, Evidence for HBr production due to minor channel branching at mid-latitu des, *Geophys. Res. Lett.,25,* 55-58, 1998.

Croteau, P. C., An assesment of the Canadian Middle Atmosphere model (CMAM) using satellite observations, M.Sc. thesis, York Univ., Toronto, Ont., Canada, 1998.

de Grandpré, J., J. W. Sandilands, J. C. McConnell, S. R. Beagley, P. C. Croteau, and M. Y. Danilin, Canadian Middle Atmosphere Model: Preliminary results from the Chemical Transport Module, *Atmos. Ocean, 35,* 385-431, 1997.

DeMore, W. B., S. P. Sander, D. M. Golden, R. F. Hampson, M. J. Kurylo, C. J.Howard, A. R. Ravishankara, C. E. Kolb, and M. J. Molina, Chemical kinetics and photochemical data for use in stratospheric modeling, JPL Pub., *94-26,* 1994.

DeMore, W. B., S. P. Sander, D. M. Golden, R. F. Hampson, M. J. Kurylo, C. J. Howard, A. R. Ravishankara, C. E. Kolb, and M. J. Molina, Chemical kinetics and photochemical data for use in stratospheric modeling, JPL Pub., *97-4,* 1997.

Dessler, A.E., S.R. Kawa, A.R. Douglass, D.B. Considine, J.B. Kumer, A.E. Roche, J.L. Mergenthaler, J.W. Waters, J.M. Russell III, and J.C Gille, A test of the partitioning between ClO and $ClONO_2$ using simultaneous UARS measurements of ClO, NO_2 and $ClONO_2$, *J. Geophys. Res., 101,* 12,515-12,521, 1996.

Eckman, R. S., W. L. Grose, R. E. Turner, W. T. Blackshear, J. M. Russell III, L. Froidevaux, J. W. Waters, J. B. Kumer, and A. E. Roche, Stratospheric trace constituents simulated by a three-dimensional general circulation model: Comparison with UARS data, *J. Geophys. Res., 100,* 13,951-13,967, 1995.

Eckman, R. S., W. L. Grose, R. E. Turner, and W. T. Blackshear, Polar ozone depletion: A three-dimensional chemical modeling study of its long-term impact, *J. Geophys. Res., 101,* 22,977-22,989, 1996.

Fleming, E.L., S. Chandra, J.J. Barnett, and M. Corney, Zonal mean temperature, pressure, zonal wind and geopotential height as function of latitude, *Adv. Space Res., 10, No. 12,* 11-59, 1990.

Fomichev, V. I., and J.-P. Blanchet, Development of the new CCC/GCM longwave radiation model for extension into the middle atmosphere, *Atmos. Ocean, 33,* 513-529, 1995.

Fomichev, V. I., J.-P. Blanchet, and D. S. Turner, Matrix parameterization of the 15 μm CO_2 band cooling in the middle and upper atmosphere for variable CO_2 concentration, *J. Geophys. Res., 103,* 11,505-11,528, 1998.

Garcia, R. R., and B. A. Boville, "Downward control" of the mean meridional circulation and temperature distribution of the polar winter stratosphere, *J. Atmos. Sci., 51,* 2238-2245, 1994.

Hall, T. M., D. W. Waugh, K. A. Boering, and R. A. Plumb, Evaluation of transport in stratospheric models, *J. Geophys. Res., 104,* 18,815-18,839, 1999.

Holton, J. R., P. H. Haynes, M. E. McIntyre, A. R. Douglass, R. B. Rood, and L. Pfister, Stratosphere-troposphere exchange, *Rev. Geophys., 33,* 404-439, 1995.

Intergovernmental Panel on Climate Change (IPCC), Aviation and the global atmosphere, edited by J. E. Penner et al., special report. 373 pp., Cambridge Univ. Press, New York, 1999.

Jucks, K. W., D. G. Johnson, K. V. Chance, W. A. Traub, J. J. Margitan, G. B.Osterman, R. J. Salawitch, and Y. Sasano, Observations of OH, HO_2, H_2O, and O_3 in the upper stratosphere: Implications for HO_x photochemistry, *Geophys. Res. Lett., 25,* 3935-3938, 1998.

Kawabata, K. H. Ogawa, Y. Yonekura, H. Susuki, M. Susuki, Y. Iwasaka, T. Shibata, and T. Sakai, Ground-based radiometry of stratomesopheric ozone employing a superconductive receiver, *J. Geophys. Res., 102,* 1371-1377, 1997.

Keating, G. M., M. C. Pitts, and D. F. Young, Ozone reference models for the middle atmosphere, *Adv. Space Res., 10, No. 12,* 12,317-12,355, 1990.

Khosravi, R., G. P. Brasseur, A. K. Smith, D. W. Rusch, J. W. Waters, and J. M. Russell III, Significant reduction in the stratospheric ozone deficit using a three-dimensional model constrained with UARS data, *J. Geophys. Res., 103,* 16,203-16,219, 1998.

Koppers, G. A. A., and D. P. Murtagh, Model studies of the influence of O_2 photodissociation parameterizations in the Schumann-Runge bands on ozone related photolysis in the upper atmosphere, *Ann. Geophys., 14,* 68-79, 1996.

Lary, D. J., M. P. Chipperfield, R. Toumi, and T. M. Tenton, Heterogeneous atmospheric bromine chemistry, *J. Geophys. Res., 101,* 1489-1504, 1996.

McCormack, J.P., and L.L. Hood, Apparent solar cycle variations of upper stratospheric ozone and temperature: Latitude and seasonal dependences, *J. Geophys. Res., 101,* 20,933-20,944, 1996.

McElroy, M. B., and R. J. Salawitch, Changing composition of the changing stratosphere, *Science, 243,* 763-770, 1989.

McFarlane, N. A., The effect of orographically excited gravity wave drag on the general circulation of the lower stratosphere and troposphere, *J. Atmos. Sci., 44,* 1775-1800, 1987.

McFarlane, N. A., G. J. Boer, J.-P. Blanchet, and M. Lazare, The Canadian Climate Centre second generation GCM

and its equilibrium climate, *J. Clim., 5,* 1013-1044, 1992.

Medvedev, A. S., and G. P. Klaassen, Vertical evolution of gravity wave spectra and the parameterization of associated wave drag, *J. Geophys. Res., 100,* 25,841-25,853, 1995.

Medvedev, A. S., G. P. Klaassen, and S. R. Beagley, On the role of an anisotropic gravity wave spectrum in maintaining the circulation of the middle atmosphere, *Geophys. Res. Lett., 25,* 509-512, 1998.

Mlynczak, M. G., and S. Solomon, A detailed evaluation of the heating efficiency in the middle atmosphere, *J. Geophys. Res., 98,* 10,517-10,541, 1993.

Mote, P. W., K. H. Rosenlof, M. E. McIntyre, E. S. Carr, J. C. Gille, J. R Holton, J. S. Kinnersley, H. C. Pumphrey, J. M. Russell III, and J. W. Waters, An atmospheric tape recorder: The imprint of tropical tropopause temperatures on stratospheric water vapor, *J. Geophys. Res., 101,* 3989-4006, 1996.

Müller, R., and G. P. Brasseur, IMAGES: A three-dimensional chemical transport model of the global troposphere, *J. Geophys. Res.,100,* 16,445-16,490, 1995.

Pawson, S., et al., The GCM-Reality Intercomparison Project for SPARC: scientific issues and initial results, *Bull. Am. Meteorol. Soc., 81,* 781-796, 2000.

Perliski, L. M., and J. London, Satellite-observed long-term averaged seasonal and spatial ozone variations in the stratosphere, *Planet. Space Sci., 37,* 1509-1525, 1989.

Plass, G. N., G. W. Kattawar, and F. E. Catchings, Matrix operator theory of radiative transfer, 1, Rayleigh scattering, *Appl. Opt., 12,* 314-329, 1973.

Randel, W. J., J. F. Wu, J. M. Russel III, A. Roche, and J. W. Waters, Seasonal cycles and QBO variations in stratospheric CH_4 and H_2O observed in UARS HALOE data, *J. Atmos. Sci., 55,* 163-185, 1998.

Rasch, P. J., B. A. Boville, and G P. Brasseur, A three-dimensional general circulation model with coupled chemistry for the middle atmosphere, *J. Geophys. Res., 100,* 9041-9071, 1995.

Ravishankara, A. R., G. Hancock, M. Kawasaki, and Y. Matsumi, Photochemistry of ozone: Surprises and recent lessons, *Science, 280,* 60-61, 1998.

Rosenlof, K. H., and J. R Holton, Estimates of the stratospheric residual circulation using the downward control principle, *J. Geophys. Res., 98,* 10,465-10,479, 1993.

Sandilands, J. W., and J. C. McConnell, Evaluation of a reduced-jacobian numerical chemical solver, *J. Geophys. Res, 102,* 19,073-19,088, 1997.

Sandor, B. J., and R. T. Clancy, Mesospheric HO_x chemistry from diurnal microwave observations of HO_2, O_3, and H_2O, *J. Geophys. Res., 103,* 13,337-13,351, 1998.

Shindell, D., D. Rind, and P. Lonergan, Increased polar ozone losses and delayed eventual recovery owing to increasing green-house gas concentrations, *Nature, 392,* 589-592, 1998.

Summers, M. E., R. R. Conway, D. E. Siskind, M. H. Stevens, D. Offermann, M. Riese, P. Preusse, D. F. Strobel, and J. M. Russell III, Implications of satellite OH observations for middle atmospheric H_2O and ozone, *Science, 277,* 1967-1970, 1997.

Talukdar, R. K., C. A. Longfellow, M. K. Gilles, and A. R. Ravishankara, Quantum yields of $O(^1D)$ in the photolysis of ozone between 289 and 329 nm as a function of temperature, *Geophys. Res., Lett., 25,* 143-146, 1998.

Volk, C.M. et al., Quantifying transport between the tropical and mid-latitude lower stratosphere, *Science, 272,* 1763-1768, 1996.

Warneck, P., *Chemistry of the Natural Atmosphere,* 757 pp., Academic Press, San Diego, Calif., 1988.

World Meteorological Organization (WMO), *Scientific assessment of ozone depletion 1991, WMO Rep. 25,* Global Ozone Res. and Monit. Proj., Geneva, Switzerland, 1992.

World Meteorological Organization (WMO), *Scientific assessment of ozone depletion 1994, WMO Rep. 37,* Global Ozone Res. and Monit. Proj., Geneva, Switzerland, 1995.

World Meteorological Organization (WMO), *Scientific assessment of ozone depletion 1998, WMO Rep. 44,* Global Ozone Res. and Monit. Proj., Geneva, Switzerland, 1999.

Zhang, G. J., and N. A. McFarlane, Sensitivity of climate simulations to the parameterization of cumulus convection in the CCC GCM, *Atmos. Ocean, 33,* 407-446, 1995.

S. R. Beagley, J. de Grandpré, V. I. Fomichev, E. Griffioen, J. C. McConnell, and A. S. Medvedev, Department of Earth and Atmospheric Science, York University, 4700 Keele St., Toronto, Ontario, Canada M3J 1P3. (beagley@nimbus.yorku.ca; jean@nimbus.yorku.ca; victor@nimbus.yorku.ca; erik@nimbus.yorku.ca; jack@nimbus.yorku.ca; medvedev@nimbus.yorku.ca)

T. G. Shepherd, Department of Physics, University of Toronto, Toronto, Ontario, Canada M5S 1A7. (tgs@atmosp.physics.utoronto.ca)

(Received April 12, 2000; revised July 7, 2000;
accepted July 19, 2000.)